



Contents lists available at ScienceDirect

## Spectrochimica Acta Part A: Molecular and Biomolecular Spectroscopy

journal homepage: [www.elsevier.com/locate/saa](http://www.elsevier.com/locate/saa)

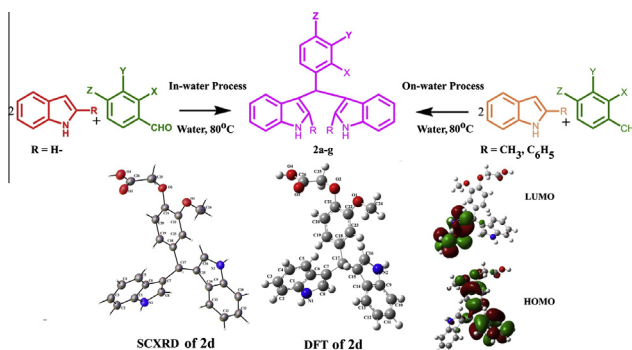
# *In situ* Bronsted–Lowry acid catalyzed syntheses, characterization, single crystal XRD, electronic spectral-, DPPH radical scavenging-, and DNA protection studies of aryl-3,3'-bis(indolyl)methanes

G.S. Suresh Kumar<sup>a</sup>, A. Antony Muthu Prabhu<sup>b</sup>, P.G. Seethalakshmi<sup>c</sup>, N. Bhuvanesh<sup>d</sup>, S. Kumaresan<sup>e,\*</sup><sup>a</sup> Faculty of Chemistry, Department of Science and Humanities, Dr. Mahalingam College of Engineering and Technology (Dr. MCET), Udumalai Road, Pollachi 642 003, Tamilnadu, India<sup>b</sup> Department of Chemistry, Manonmaniam Sundaranar University, Tirunelveli 627 012, Tamilnadu, India<sup>c</sup> Department of Chemistry, APC Mahalakshmi College for Women, Toothukkudi 628 002, Tamilnadu, India<sup>d</sup> Department of Chemistry, Texas A&M University, College Station, TX 77842, USA<sup>e</sup> Department of Chemistry, Noorul Islam University, Kumaracoil, Thuckalay 629 180, Tamilnadu, India

## HIGHLIGHTS

- Formylphenoxyacetic acids act as *in situ* Bronsted–Lowry acid catalysts for the syntheses of BIMs.
- SCXRD and DFT, the two indole rings and the phenyl ring are found to be noncoplanar.
- All the synthesized compounds display  $\pi$ – $\pi^*$  transition in solvents.
- BIMs have better DPPH radical scavenging activity.
- BIMs have better reduction of oxidative damage of DNA.

## GRAPHICAL ABSTRACT



## ARTICLE INFO

## Article history:

Received 5 December 2012

Received in revised form 24 November 2013

Accepted 5 December 2013

Available online 18 December 2013

## Keywords:

3,3'-Bis(indolyl)methanes

Crystal structure

Density functional theory

DPPH radical scavenging

DNA protection

## ABSTRACT

A series of novel aryl-3,3'-bis(indolyl)methanes (BIMs) were synthesized using indole and formylphenoxyacetic acid(s) in water in the absence of any catalyst. The formylphenoxyacetic acid behaves as an *in situ* Bronsted–Lowry acid catalyst in water. UV–Visible and fluorescence spectra of the compounds were recorded in selected solvents. The gas phase geometry optimization of the compounds were achieved using DFT calculations at B3LYP/3-21G(+) level of theory. The electronic properties, such as HOMO–LUMO energies were calculated using the above method based on the optimized structure. Compounds have better DPPH radical scavenging activity and reduction of oxidative damage of DNA.

© 2013 Elsevier B.V. All rights reserved.

## Introduction

Bis(indolyl)methanes (BIMs) have received more attention due to their bioactivities against human pathogens [1]. BIMs reveal

antimicrobial-, antifungal-, antibiotic-, antibacterial-, antiangiogenic-, cytotoxic-, antimetastatic-, analgesic-, anti-inflammatory-, etc. activity. Furthermore, BIMs are used in dyes, laser technologies, and fluorescent materials for visualization of biomolecules [2]. There is a continuous search for the formulation of newer synthetic entities of BIMs via efficient methods due to their versatile application possibilities.

\* Corresponding author. Tel.: +91 9443182502.

E-mail address: [skumarmsu@yahoo.com](mailto:skumarmsu@yahoo.com) (S. Kumaresan).

Aryloxyaliphatic acid derivatives possess an extensive range of diverse bioactivities such as antimicrobial-, anti-inflammatory-, antioxidant-, antibacterial-, analgesic-, antisickling-, anti-paemic-, antiplatelet-, non-prostanoid prostacyclin mimetic-, diuretic-, and growth regulators [3].

In the ideal case, a target molecule is prepared from readily available starting materials in one simple, safe, environment-friendly operation that proceeds quickly and in reasonable yield [4]. Water finds an important place in organic syntheses as solvent because of its abundance and less toxicity [5]. Water-facilitated reactions are categorized as 'in-water process' and 'on-water process' based on the starting materials and reaction conditions [6].

Fundamental understanding on structural and energetic properties of this kind of materials could lead to beneficial knowledge for the design of novel bisarylmethanes. Therefore, it is of interest to discuss the geometrical and the electronic properties based on density functional theory (DFT) which is shown as a favorite among several computational chemistry methods because of its great accuracy in reproducing the experimental values in molecular geometry, vibrational frequencies, atomic charges, dipole moment etc. [7].

To the best of our knowledge, we have not encountered any report regarding the use of aromatic aldehydes bearing carboxylic acid group in the side chain acting as an *in situ* acid catalyst for the formation of BIMs in water. This deliberated us to carry out the efficient syntheses of BIMs from indole and formylphenoxyacetic acid(s) at elevated temperature in water in the absence of any external acid catalyst. In continuation of our work in organic syntheses [2b,3b,3c], herein we report the syntheses, the geometrical parameters studied by both single crystal XRD and theoretical calculations, the fluorescence activity in selected solvents, DPPH radical scavenging activity, and DNA strand breakage assay of BIMs.

## Experimental

### General methods

Melting points were measured in open capillary tubes and are uncorrected. The crystal structure was determined using a Bruker APEX 2 X-ray (three-circle) diffractometer. The  $^1\text{H}$  NMR and  $^{13}\text{C}$  NMR spectra were recorded on a Bruker (Avance) 500 MHz NMR instrument using TMS as internal standard and  $\text{CDCl}_3$  as solvent. Standard Bruker software was used throughout. Chemical shifts are given in parts per million ( $\delta$  scale) and the coupling constants in Hertz. Infrared spectra were recorded on a JASCO FT-IR Model 410 spectrophotometer (in KBr pellet). Band positions are reported in reciprocal centimetres ( $\text{cm}^{-1}$ ). Absorption measurements were carried out with a Shimadzu UV 1601 PC model UV-Visible spectrophotometer and fluorescence measurements were made by using a Shimadzu spectrofluorimeter model RF-5301. Silica gel-G plates (Merck) were used for TLC analysis with a mixture of chloroform and methanol as eluent. The electrospray (ESI) mass spectra were recorded on a THERMO Finnigan LCQ Advantage max ion trap mass spectrometer. Samples (10  $\mu\text{L}$ ) (dissolved in solvent such as methanol/acetonitrile/water) were introduced into the ESI source through Finnigan surveyor autosampler. Elemental analyses were performed on a Perkin Elmer 2400 Series II Elemental CHNS analyzer. Formylphenoxyacetic acids were synthesized by literature method [3b].

### Syntheses of BIMs acids

Formylphenoxyaliphatic acid (2.5 mmol) was dissolved in water (10 mL) at 80 °C, indole (5 mmol) was added with vigorous stirring at 80 °C for 5–10 min. After the completion of starting

materials (monitored by TLC, chloroform:methanol), the reaction mixture was cooled to room temperature, the solid was filtered, washed with water, dried well and recrystallized from hot ethanol.

### 2-{2-[Bis(1H-indol-3-yl)methyl]phenoxy}acetic acid (2a)

Pink solid; 84%; m.p. 130–132 °C; IR (KBr): 3402, 1723  $\text{cm}^{-1}$ ;  $^1\text{H}$  NMR (500 MHz,  $\delta$  ppm): 4.53 (s, 2H), 6.41 (s, 1H), 6.46–9.16 (m, 14H), 9.16 (s, 2H);  $^{13}\text{C}$  NMR (125 MHz,  $\delta$  ppm): 32.4, 66.1, 101.7, 111.1, 111.3, 112.3, 118.5, 118.7, 119.3, 119.9, 120.4, 121.2, 121.4, 124.0, 124.5, 127.0, 127.2, 130.0, 133.6, 136.8, 155.5, 171.1; ESI-MS: 395.50; Anal. Calcd. for  $\text{C}_{25}\text{H}_{20}\text{N}_2\text{O}_3$ : C, 75.74; H, 5.08; N, 7.07%. Found: C, 75.72; H, 5.06; N, 7.10%.

### 2-{2-[Bis(1H-indol-3-yl)methyl]-6-methoxyphenoxy}acetic acid (2b)

Pink solid; 86%; m.p. 138–140 °C; IR (KBr): 3408, 1731  $\text{cm}^{-1}$ ;  $^1\text{H}$  NMR (500 MHz,  $\delta$  ppm): 3.89 (s, 3H), 4.19 (s, 2H), 6.22 (s, 1H), 6.55–7.40 (m, 13H), 7.64 (s, 2H);  $^{13}\text{C}$  NMR (125 MHz,  $\delta$  ppm): 33.6, 55.8, 71.2, 102.6, 110.1, 111.0, 111.2, 118.6, 119.4, 119.6, 119.8, 120.7, 122.0, 122.1, 123.5, 124.1, 125.0, 126.8, 127.8, 136.7, 138.0, 145.2, 151.2, 170.6; ESI-MS: 426.42; Anal. Calcd. for  $\text{C}_{26}\text{H}_{22}\text{N}_2\text{O}_4$ : C, 73.23; H, 5.20; N, 6.57%. Found: C, 73.25; H, 5.25; N, 6.60%.

### 4-{2-[Bis(1H-indol-3-yl)methyl]phenoxy}acetic acid (2c)

Pink solid; 84%; m.p. 145–147 °C; IR (KBr): 3406, 1760  $\text{cm}^{-1}$ ; ESI-MS: 395.45; Anal. Calcd. for  $\text{C}_{25}\text{H}_{20}\text{N}_2\text{O}_3$ : C, 75.74; H, 5.08; N, 7.07%. Found: C, 75.78; H, 5.12; N, 7.04%.

### 4-{2-[Bis(1H-indol-3-yl)methyl]-6-methoxyphenoxy}acetic acid (2d)

Pink solid; 86%; m.p. 159–161 °C; IR (KBr): 3406, 1760  $\text{cm}^{-1}$ ;  $^1\text{H}$  NMR (500 MHz,  $\delta$  ppm): 3.72 (s, 3H), 4.59 (s, 2H), 5.80 (s, 1H), 6.48–7.40 (m, 13H), 9.34 (s, 2H);  $^{13}\text{C}$  NMR (125 MHz,  $\delta$  ppm): 4.75, 60.5, 71.0, 106.4, 116.0, 117.6, 118.4, 123.3, 123.8, 123.9, 124.3, 125.1, 125.3, 126.0, 126.1, 128.6, 129.9, 131.7, 132.5, 141.5, 143.5, 150.3, 153.8, 175.8; ESI-MS: 426.42; Anal. Calcd. for  $\text{C}_{26}\text{H}_{22}\text{N}_2\text{O}_4$ : C, 73.23; H, 5.20; N, 6.57%. Found: C, 73.25; H, 5.25; N, 6.60%.

### 2-{2-[Bis(2-methyl-1H-indol-3-yl)methyl]phenoxy}acetic acid (2e)

Pink solid; 78%; m.p. 122–126 °C; IR (KBr): 3395, 1727  $\text{cm}^{-1}$ ;  $^1\text{H}$  NMR (500 MHz,  $\delta$  ppm): 2.12 (s, 6H), 4.37 (s, 2H), 6.12 (s, 1H), 6.78–7.51 (m, 12H), 7.83 (s, 2H);  $^{13}\text{C}$  NMR (125 MHz,  $\delta$  ppm): 12.2, 33.6, 66.3, 100.1, 110.0, 110.3, 110.5, 112.4, 112.6, 118.8, 119.1, 119.5, 120.2, 120.7, 120.9, 121.6, 125.2, 127.3, 129.0, 130.4, 132.0, 133.2, 135.1, 135.2, 136.1, 137.4, 156.1, 170.8; ESI-MS: 424.00; Anal. Calcd. for  $\text{C}_{27}\text{H}_{24}\text{N}_2\text{O}_3$ : C, 76.39; H, 5.70; N, 6.60%. Found: C, 76.42; H, 5.66; N, 6.62%.

### 2-{2-[Bis(2-methyl-1H-indol-3-yl)methyl]-6-methoxyphenoxy}acetic acid (2f)

Pink solid; 76%; m.p. 148–150 °C; IR (KBr): 3389, 1725  $\text{cm}^{-1}$ ;  $^1\text{H}$  NMR (500 MHz,  $\delta$  ppm): 2.09 (s, 6H), 3.87 (s, 3H), 3.91 (s, 2H), 6.17 (s, 1H), 6.81–7.29 (m, 11H), 7.50 (s, 2H);  $^{13}\text{C}$  NMR (125 MHz,  $\delta$  ppm): 12.7, 13.7, 33.7, 55.7, 69.1, 99.7, 110.2, 110.4, 112.6, 118.5, 119.1, 119.2, 119.3, 119.9, 120.4, 122.5, 123.6, 129.0, 132.3, 135.2, 136.2, 138.4, 152.3, 171.1; ESI-MS: 453.50; Anal. Calcd. for  $\text{C}_{28}\text{H}_{26}\text{N}_2\text{O}_4$ : C, 73.99; H, 5.77; N, 6.16%. Found: C, 74.02; H, 5.76; N, 6.19%.

### 2-[2-[Bis(2-phenyl-1H-indol-3-yl)methyl]phenoxy]acetic acid (2g)

Green solid; 72%; m.p. 202–204 °C; IR (KBr): 3622, 3424, 1725 cm<sup>-1</sup>; <sup>1</sup>H NMR (500 MHz, δ ppm): 3.72 (s, 2H), 6.22 (s, 1H), 6.75–7.68 (m, 22H), 8.12 (s, 2H), 10.26 (s, 1H); <sup>13</sup>C NMR (125 MHz, δ ppm): 34.8, 66.3, 70.2, 110.9, 113.1, 114.8, 118.8, 120.9, 121.5, 125.3, 126.9, 127.5, 128.0, 128.4, 128.8, 129.1, 130.9, 133.4, 136.1, 156.3, 170.9; ESI-MS: 547.63; Anal. Calcd. for C<sub>37</sub>H<sub>28</sub>N<sub>2</sub>O<sub>3</sub>: C, 81.00; H, 5.14; N, 5.11%. Found: C, 81.02; H, 5.16; N, 5.10%.

### Ethyl 2-[2-[bis(1H-indol-3-yl)methyl]phenoxy]acetate (4b)

Pale pink solid; 77%; mp = 176–178 °C; IR (KBr): 3401, 1749 cm<sup>-1</sup>; <sup>1</sup>H NMR (300 MHz, δ ppm): 1.22 (t, *J* = 14.1 Hz, 3H), 4.18 (q, *J* = 21.3 Hz, 3H), 4.58 (s, 2H), 6.43 (s, 1H), 6.55 (s, 2H), 6.78–6.87 (m, 2H), 6.98 (t, *J* = 7.8 Hz, 2H), 7.11–7.17 (m, 4H), 7.34 (d, *J* = 9.0 Hz, 2H), 7.44 (d, *J* = 7.8 Hz, 2H), 7.84 (s, 2H); <sup>13</sup>C NMR (75 MHz, CDCl<sub>3</sub>): 14.0, 32.5, 61.0, 66.2, 110.8, 112.0, 119.0, 119.4, 120.1, 121.5, 121.7, 123.5, 127.0, 127.2, 130.0, 133.2, 136.8, 155.8, 169.1; ESI-MS: *m/z* 424.3; Anal. Calcd. for C<sub>27</sub>H<sub>24</sub>N<sub>2</sub>O<sub>3</sub>: C, 76.39; H, 5.70; N, 6.60%. Found: C, 76.45; H, 5.7; N, 6.55%.

### Computational methods

The ground state geometries of BIMs 2a–d were optimized by using the Gaussian-09 series of programs [8]. For this purpose the B3LYP/DFT approach, which includes the interchange hybrid functional from Becke (B3) [9a] in combination with the three-parameter correlation functional by Lee–Yang–Parr (LYP) [9b] was employed in combination with the basis set 3-21G(\*).

### Evaluation of radical scavenging activity using DPPH model system

The radical scavenging activity of the compounds was evaluated as per the method of Blois [10] with slight modification [11]. The compounds (2a–d) and BHA at different concentrations (25, 50, 75 and 100 ppm in 1 mL) were taken in different test tubes. Four milliliters of 0.1 mM methanolic solution of DPPH was added to these tubes and shaken vigorously. The tubes were allowed to stand at 27 °C for 20 min. The control was prepared as above without any compound and methanol was used for the baseline correction. Optical density (OD) of the samples was measured at 517 nm. Radical scavenging activity was expressed as the inhibition percentage and was calculated using the following formula:

$$\% \text{Radical scavenging activity} = (\text{Control OD} - \text{Sample OD} / \text{Control OD}) \times 100.$$

### DNA strand breakage assay

The DNA strand breakage assay was carried out by an established method [12]. Briefly, each reaction mixture contained 10 μL of DNA (calf thymus, pBR 322 or pUC 18), 10 μL of 1 mM FeSO<sub>4</sub>, 10 μL of 10 mM H<sub>2</sub>O<sub>2</sub>, and 10 μL of compound (2a–d, 4a and b); the volume was brought to 100 μL with PBS. The mixtures were incubated for 60 min in a vial at 37 °C. 5 μL of the reaction mixtures were mixed with 2 μL of gel loading solution (0.1 M EDTA, 0.5% sodium dodecyl sulfate, 40% sucrose, and 0.5% bromophenol blue) and loaded into individual wells in a 0.8% agarose gel for electrophoresis at 5 V/cm in TBE buffer (0.1 M Tris; 0.09 M boric acid; 0.001 M EDTA). The gel was visualized by photographing the fluorescence of intercalated ethidium bromide under a UV illuminator.

## Results and discussion

### Syntheses of phenoxyaliphatic acids of 3,3'-BIMs

Synthesis of 2-[2-[bis(1H-indol-3-yl)methyl]phenoxy]acetic acid (2a) using indole and formylphenoxyacetic acid (1a) in water was taken as the model reaction. Synthesis of 2-[2-[bis(1H-indol-3-yl)methyl]phenoxy]acetic acid (2a) using indole and formylphenoxyacetic acid (1a) in water was achieved in 84% yield at 80 °C in the absence of any acid catalyst. Formylphenoxyacetic acid and indole were completely miscible in hot water and a pink solid was precipitated out within 5 min. This reaction was categorized as 'in-water process' [3f,6] (Scheme 1).

The above *in situ* Bronsted–Lowry acid catalyzed reaction [3f,13] was checked using ethyl 2-formylphenoxyacetate as well as the sodium salt of 2-formylphenoxyacetic acid. Formation of 4a, 4b, and 4c from the condensation of indole with the corresponding aldehyde(s) in water at 80 °C was not possible in these cases even after 12 h. But the same reaction proceeded smoothly in the presence of acetic acid (pK<sub>a</sub> 4.76) in water to afford 4a, 4b, and 2a (*vide* supporting information, Scheme II). This manifests the formation of hydronium ion from 2-formylphenoxyacetic acid (pK<sub>a</sub> 3.04) for the synthesis of 2a in water.

Thus it could be confirmed that the syntheses of BIMs using formylphenoxyacetic acid(s) did not require any external acid catalyst. Formylphenoxyacetic acid(s) itself acted as a Bronsted–Lowry acid catalyst in water. To demonstrate the generality of this methodology, the replacement of indole with 2-methylindole and 2-phenylindole was studied (Scheme 1). Under the same reaction conditions, 2-methylindole and 2-phenylindole afforded the BIMs *via* 'on-water process'. Even the hydrophobicity of these indoles did not forbid the formation of the corresponding BIMs in moderate yields. This is due to the strong Bronsted–Lowry acid strength of the formylphenoxyacetic acid. Synthesis of 2-phenylindole-substituted BIM 2g using this aldehyde substantiates that the corresponding formylphenoxyacetic acid is a better Bronsted–Lowry acid than acetic acid in water. Hence the mechanism is proposed for the formation of 2a from the condensation of 2-formylphenoxyacetic acid and indole (*vide* supporting information, Fig. s1).

To further investigate the synthetic potential of this process, the *in situ* Bronsted–Lowry acid catalyzed reaction was extended to phenolic aldehydes in water. We examined the synthesis of [bis(1H-indol-3-yl)methyl]phenols (5) from indole and hydroxybenzaldehyde(s) in the absence of acid catalyst in water. After 1 h, the corresponding BIMs were observed in moderate yields (5a, 65% and 5b, 68%). Hydroxybenzaldehydes were not completely miscible in hot water. This reaction was regarded as 'on-water process' (*vide* supporting information, Scheme III). The increase in reaction time and lower yield are due to the less acidic nature of hydroxybenzaldehydes (pK<sub>a</sub> for 5a, 6.79 and 5b, 7.66) in water.

Further, we have subjected the four acid derivatives 2a–d of BIMs for characterizing their structural-, photophysical-, radical scavenging activity, and DNA strand breakage studies. The optimized structures of the selected derivatives with the substitutions –OCH<sub>2</sub>COOH at *o*-/*p*-positions and –OCH<sub>3</sub> group at *m*-position in the phenyl ring are given in supporting information, Fig. s2.

### Single crystal XRD studies

The molecular structure of the derivative 2d has been determined by single crystal X-ray diffraction (CCDC No. 911716) and the ORTEP diagram is shown in Fig. 1. The crystal data and structural refinement of 2d are summarized in Table 1. The derivative 2d was crystallized as a triclinic system in methanol under dark

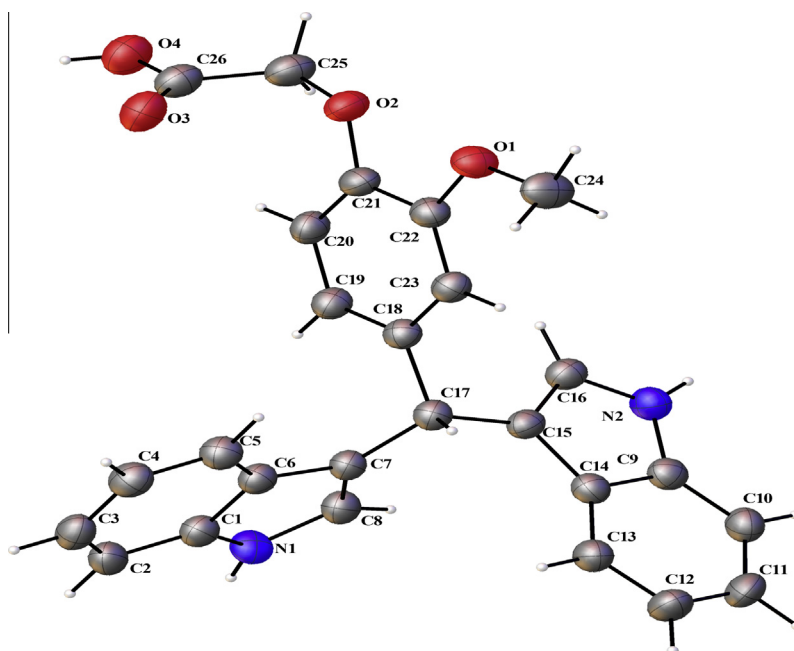
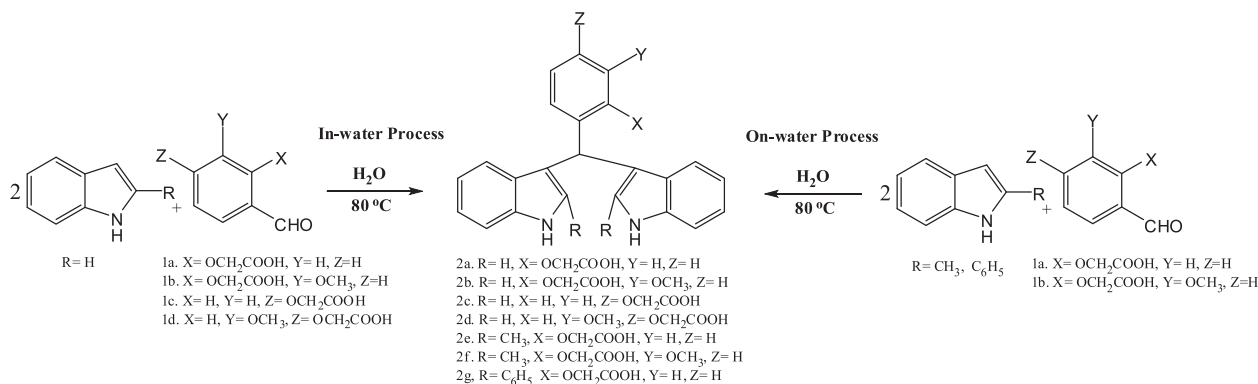


**Fig. 1.** ORTEP view of 2d.

conditions. Selected bond lengths, bond angles, and torsion angles for 2d are listed in Table 2.

In the crystal structure of compound 2d, two molecules of 2d are connected together through H-bonding (O4–H4A···O3, 1.794 Å) like a normal acid dimer synthon with the Etter's graph set notation  $R_2^2(8)$ . C–H··· $\pi$  and N–H··· $\pi$  interactions were observed. Similar interactions are found in 3,3'-BIMs derivatives [2b,14], other indole derivatives [15], and globular proteins [16]. These interactions may afford stability and contribute to the folding process or have a functional role in proteins and DNA. The dihedral angle between two indole rings is 72.79 Å, aryl ring – indole (1) is 89.41 Å, and aryl ring – indole (2) is 84.36 Å.

#### Solvent effects on absorption and fluorescence spectrum

Fig. 2 shows a typical example of the solvent effect on the electronic absorption and emission spectrum of compound 2d. The absorption and fluorescence spectra of 2a, 2b, and 2c are almost similar to those of 2d. The absorption and emission wavelengths and Stokes shift of BIMs (2a–d) in selected solvents (cyclohexane, acetonitrile, methanol, and water) are presented in Table 3. In

the exploited wavelength region (200–800 nm), all compounds showed an absorption peak at 290 nm. The molecules showed a high extinction coefficient of the order of  $10^4 \text{ M}^{-1} \text{ cm}^{-1}$  at the lowest energy transition in the solvents. The substituent  $-\text{OCH}_2\text{COOH}$  at *o*- and *p*-position; and  $-\text{OCH}_3$  group at *m*-position have little influence on the absorption wavelength and absorbance. However, there is not much change in the energy of transition in the different solvents, which implies that solvent stabilization of the ground state species is not significant in all compounds [17].

The fluorescence spectra of compounds were measured at room temperature in cyclohexane, acetonitrile, methanol, and water as shown in Fig. 2. Compounds 2a–d excited at 290 nm in solvents showing the maximum emission peak around 340 nm. Unlike absorption spectra, this implies that the substituent of the phenyl group has a significant change on the fluorescence wavelength and fluorescence intensity of the compounds. The red shift on the fluorescence spectra on changing the solvent from cyclohexane to water indicates the effect of hydrogen bonding in the excited state of the compounds [18].

The absorption and emission spectra of the compounds mainly originate from the indole rings. The presence of a methine group in

**Table 1**  
Crystal data and structure refinement of 2d.

Empirical formula	C <sub>27</sub> H <sub>24</sub> N <sub>2</sub> O <sub>3</sub>
CCDC No.	911716
Formula weight	424.48
Temperature	110(2) K
Wavelength	0.71073 Å
Crystal system	Monoclinic
Space group	P2(1)/c
Unit cell dimensions	
<i>a, b, c</i> (Å)	9.6067(11), 13.9907(15), 16.2903(18)
$\alpha, \beta, \gamma$ (°)	90°, 95.91(10)°, 90°
Volume	2177.8(4) Å <sup>3</sup>
Z	4
Density (calculated)	1.295 Mg/m <sup>3</sup>
Absorption coefficient	0.085 mm <sup>-1</sup>
<i>F</i> (000)	896
Crystal size	0.58 × 0.22 × 0.16 mm <sup>3</sup>
Theta range for data collection	2.13–27.50°
Index ranges	−12 ≤ <i>h</i> ≤ 12, −18 ≤ <i>k</i> ≤ 18, −20 ≤ <i>l</i> ≤ 20
Reflections collected	24448
Independent reflections	4955 [ <i>R</i> (int) = 0.0317]
Completeness to theta = 27.50°	99.1%
Absorption correction	Semi-empirical from equivalents
Max. and min. transmission	0.9865 and 0.9524
Refinement method	Full-matrix least-squares on <i>F</i> <sup>2</sup>
Data/restraints/parameters	4955/0/290
Goodness-of-fit on <i>F</i> <sup>2</sup>	1.045
Final <i>R</i> indices [ <i>I</i> > 2σ( <i>I</i> )]	<i>R</i> 1 = 0.0407, <i>wR</i> 2 = 0.0951
<i>R</i> indices (all data)	<i>R</i> 1 = 0.0508, <i>wR</i> 2 = 0.1014
Largest diff. peak and hole	0.276 and −0.211 eÅ <sup>-3</sup>

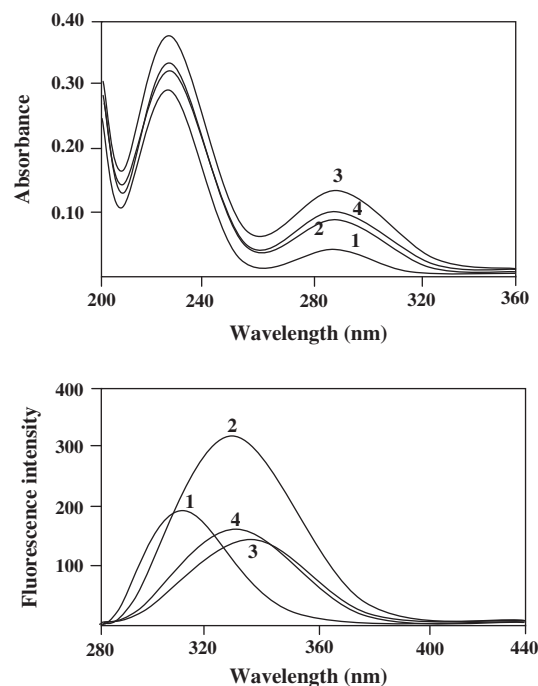
**Table 2**  
Selected bond lengths and bond angles of 2a–d.

Atom numbering	Experimental		DFT		
	2d	2d	2a	2b	2c
<b>Bond length</b>					
C17–C15	1.513(3)	1.515	1.517	1.515	1.515
C17–C18	1.518(3)	1.535	1.534	1.534	1.534
C17–C7	1.508(3)	1.518	1.520	1.517	1.518
N1–C8	1.388(3)	1.397	1.397	1.397	1.397
N2–C16	1.379(3)	1.397	1.397	1.399	1.397
C22–O1	1.378(3)	1.384	–	–	–
C20–O4	–	–	–	1.413	–
C21–O2	1.374(3)	1.394	–	–	1.397
C19–O1	–	–	1.398	1.412	–
C26–O3	1.218(3)	1.218	–	–	1.225
C25–O2	–	–	1.220	1.224	–
O2–C25	1.420(3)	1.384	–	–	1.370
O3–C25	–	–	1.379	1.376	–
O1–C24	1.422(3)	1.458	–	–	–
O4–C26	1.307(3)	–	–	1.485	–
<b>Bond angle</b>					
C7–C17–C15	112.4(2)	111.33	113.04	110.53	111.58
C7–C17–C18	113.11(19)	110.14	109.01	109.01	110.33
C15–C17–C18	110.6(2)	112.24	112.32	112.34	111.71
<b>Torsion angle</b>					
C8–C7–C17–C18	−15.74	−14.87	−73.73	−17.78	−10.98
C7–C17–C18–C23	−81.88	−83.35	−92.19	−78.14	85.99
C15–C17–C18–C19	−32.60	−30.47	−39.74	−22.62	−38.74
C16–C15–C17–C18	116.60	114.29	134.90	100.13	113.88

between the two indole rings and substituted phenyl ring prevents the extension of conjugation. The absorption and emission maxima are thus very close to that of an individual indole ring.

#### Ground state geometries at the B3LYP level

The optimized structure of the compounds was calculated at the B3LYP/3-21G(\*) level of theory by DFT method in the gas phase, carried out from the experimental structures. The geometric parameters and corresponding experimental values of 2d are listed

**Fig. 2.** Absorption and fluorescence spectra of 2d in selected solvents. 1. Cyclohexane, 2. Acetonitrile, 3. Methanol, and 4. Water.

in Table 2. The calculated geometric parameters (Table 2) represent good correlations with single crystal XRD data and can be used as a source to calculate other parameters such as total energy,  $E_{\text{HOMO}}$ ,  $E_{\text{LUMO}}$ , and dipole moment for the compound. Similarly, the ground-state geometric parameters (bond lengths and bond angles) of compounds 2a–d are very similar to each other.

**Table 3**  
Spectral properties of compounds 2a–d.

Compounds	Solvent	$\lambda_{\text{max}}$	$\log \epsilon$	$\lambda_{\text{flu}}$	Stokes shift	
2a	Cyclohexane	288.2	3.11	328	4211	
		219.6	3.42			
	Acetonitrile	290.4	3.50	345	5450	
		236.1	4.12			
	Methanol	291.6	3.59	349	5640	
		234.0	4.07			
	Water	290.2	3.38	350	5887	
		230.6	4.15			
	2b	Cyclohexane	287.2	2.23	329	4423
			219.1	3.22		
		Acetonitrile	289.0	3.60	341	5277
			235.8	4.31		
Methanol		290.3	3.65	345	5462	
		233.8	4.34			
Water		290.8	3.48	350	5816	
		231.6	4.24			
2c		Cyclohexane	287.7	2.57	327	4177
			219.5	3.40		
		Acetonitrile	289.2	3.61	340	5167
			228.6	4.26		
	Methanol	290.2	3.69	344	5389	
		230.5	4.38			
	Water	291.9	3.45	350	5687	
		235.3	4.20			
	2d	Cyclohexane	286.7	2.66	328	4392
			220.4	3.65		
		Acetonitrile	288.8	3.76	348	5891
			234.6	4.32		
Methanol		289.4	3.81	349	5901	
		234.0	4.40			
Water		290.4	3.62	351	5945	
		235.3	4.30			

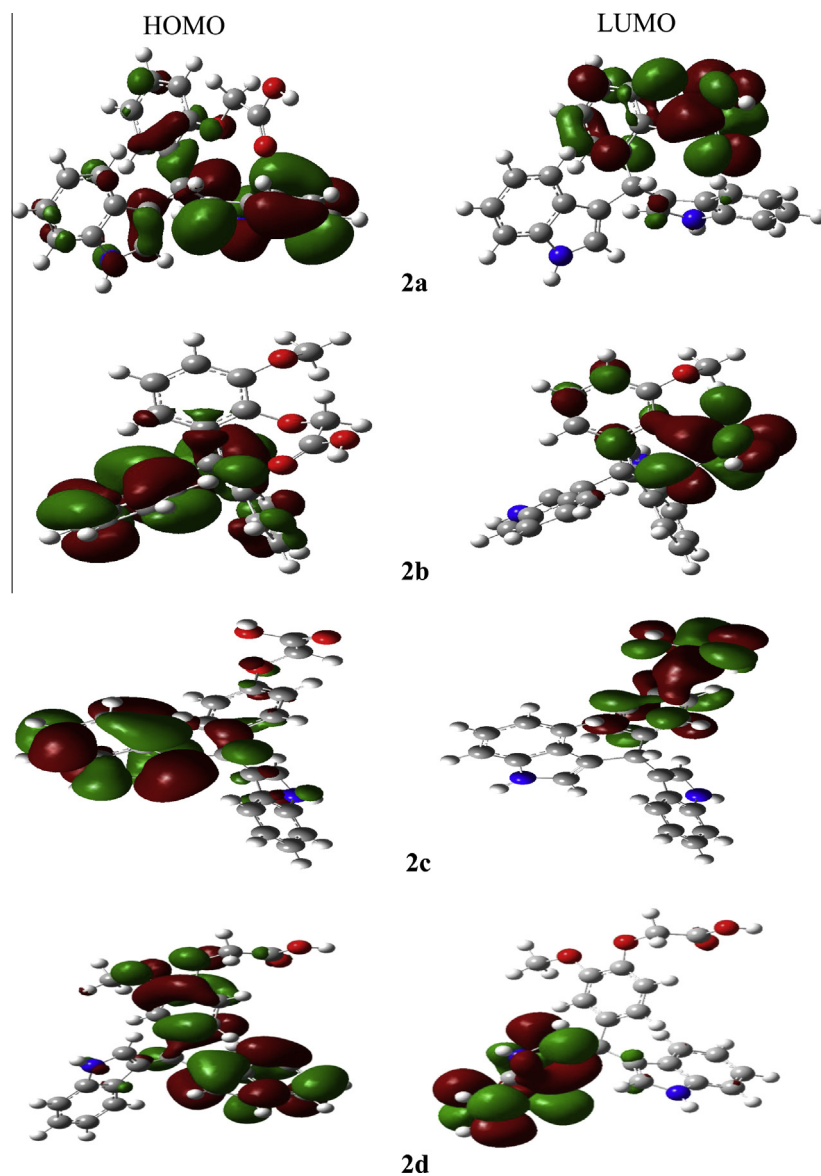


Fig. 3. Molecular orbital surfaces for the HOMO and LUMO of 2a–d computed by B3LYP/3-21G(\*) method in gas-phase.

Table 4 presents the total energies, frontier molecular orbital energies, and dipole moments of the compounds in gas phase. Obtained energy values are  $-811200$  kcal/mol for 2a,  $-882674$  kcal/mol for 2b,  $-811200$  kcal/mol for 2c, and  $-882667$  kcal/mol for 2d. From Table 4, it is understood that the substituent  $-\text{OCH}_2\text{COOH}$  present at ortho/para position of the phenyl ring exhibits higher energy (2a and 2c) compared to  $-\text{OCH}_3$  substituent in the phenyl ring of compounds 2b and 2d.

The highest occupied molecular orbital (HOMO) and lowest unoccupied molecular orbital (LUMO) of the derivatives are shown in Fig. 3. The LUMO as an electron acceptor represents the ability to accept an electron and HOMO represents the ability to donate electron. Moreover, a lower HOMO–LUMO energy gap explained the eventual stability of the compound. Further the  $(E_{\text{HOMO}}-E_{\text{LUMO}})$  gap is an important scale of stability [19] and compounds with lower  $(E_{\text{HOMO}}-E_{\text{LUMO}})$  values tend to have higher kinetic stability and lower chemical reactivity. So we have investigated the electronic structure of the compounds with these considerations using DFT method. The electron density of LUMO for 2a, 2b, and 2c is located mainly on the  $-\text{OCH}_2\text{COOH}$  group and very little

amount in phenyl ring, while the electron density of HOMO is located on one of the indole rings. However, 2d has the electron density of LUMO located on the indole ring, while the electron density of HOMO is located on the indole and phenyl rings. The energy gap value of compound 2d is more negative than other three compounds. This result suggests that 2d is more stable than 2a, 2b and 2c. Consequently, these systems present a small HOMO–LUMO gap, enabling lesser electron-transfer process in all molecules [20]. Compound 2d has a larger dipole moment than the other compounds.

Table 4

Calculated energies, frontier orbital energies, and dipole moments of 2a–d in gas phase.

	2a	2b	2c	2d
Energy (kcal/mol)	$-811200$	$-882674$	$-811200$	$-882667$
$E_{\text{HOMO}}$ (eV)	$-5.05$	$-5.03$	$-5.30$	$-5.21$
$E_{\text{LUMO}}$ (eV)	$-0.18$	$-0.10$	$-0.35$	$-0.02$
$E_{\text{HOMO}}-E_{\text{LUMO}}$ (eV)	$-4.87$	$-4.93$	$-4.94$	$-5.18$
Dipole moment (D)	1.66	3.30	2.81	4.03

**Table 5**  
DPPH radical scavenging activity of 2a–d and 4b.

Samples	Radical Scavenging Activity at different concentration (ppm)			
	25	50	75	100
2a	92.84 ± 0.83 <sup>d</sup>	90.23 ± 4.41 <sup>b</sup>	95.57 ± 1.22 <sup>b</sup>	94.04 ± 1.22 <sup>b</sup>
2b	52.38 ± 4.00 <sup>a</sup>	74.76 ± 8.38 <sup>a</sup>	71.07 ± 17.59 <sup>a</sup>	66.91 ± 6.93 <sup>a</sup>
2c	70.39 ± 2.26 <sup>c</sup>	84.02 ± 5.03 <sup>a,b</sup>	93.96 ± 3.07 <sup>b</sup>	91.95 ± 2.82 <sup>b</sup>
2d	56.43 ± 1.32 <sup>b</sup>	76.21 ± 3.25 <sup>a</sup>	87.00 ± 1.11 <sup>b</sup>	88.27 ± 2.38 <sup>b</sup>
4b	55.23 ± 1.43 <sup>b</sup>	75.76 ± 8.18 <sup>a</sup>	85.04 ± 5.00 <sup>a,b</sup>	87.30 ± 1.11 <sup>b</sup>
BHA	93.81 ± 0.01 <sup>d</sup>	90.85 ± 0.89 <sup>b</sup>	96.58 ± 0.19 <sup>b</sup>	95.04 ± 0.13 <sup>b</sup>

<sup>a,b,c,d</sup> Values are mean ± SD of triplicate values; values not having similar superscripts in the same column are significantly ( $P \leq 0.05$ ) different.

**Table 6**  
DNA protection of compounds 2a–d and 4a–b.

Lane	Samples	Calf thymus DNA	pBR 322 DNA	pUC 18 DNA
3	4b	No protection	No protection	Partial protection
4	4a	Smear	Smear	Smear
5	2a	Smear	Smear	Partial protection
6	2b	Smear	Smear	Partial protection
7	2c	Smear	Smear	Partial protection
8	2d	Smear	Smear	Partial protection

Both the HOMOs and the LUMOs are mostly  $\pi$ -antibonding type orbitals and thus, the electronic transitions from the highest occupied molecular orbital (HOMO) to the lowest unoccupied molecular orbital (LUMO) are mainly derived from the contribution of  $\pi$ - $\pi^*$  bands.

#### DPPH radical scavenging assay

The free radical scavenging activity of the compounds was tested using DPPH model system, and the results are presented in Table 5. It reveals that 25 ppm concentration of 2a has a better scavenging activity (92.84 ± 0.83) and has nearly the same as BHA, followed by 2c. Methoxy group in the *meta*-position reduces the scavenging activity compared to its unsubstituted counterparts.

#### DNA protection studies

We checked the DNA protection ability of compounds (2a–d, 4a, and 4b) with oxidatively damaged calf thymus DNA, pBR 322 DNA, and pUC 18 DNA (*vide supporting information for the electrophoresis images of calf thymus DNA, pBR 322 DNA, and pUC 18 DNA with compounds*). Hydroxyl radicals generated by the Fenton reagent are capable of oxidizing DNA and causing strand breaks, resulting in DNA fragmentation.

Gel electrophoresis of calf thymus DNA exposed to the Fenton reagent has completely cleaved the DNA. But calf thymus DNA exposed to the Fenton reagent is protected from hydroxyl radical-mediated fragmentation when incubated with compounds 2a–d and 4a except 4b. This is observed as smearing.

pBR 322 DNA exposed to Fenton reagent formed smear while electrophoresis, but pBR 322 DNA was treated with compounds 2a–d showed protection with smear equal to the DNA band (untreated).

Compounds 2a–d and 4b have partial protection against pUC 18 DNA and showed a clear band after being treated with hydroxyl radical. Table 6 reveals that the compound 4b showed complete breakage of calf thymus and pUC 322 DNA and the compounds 2a–d have better ability to protect DNA from oxidative damage compared to other compounds. The ability of compounds to protect DNA can be attributed to their scavenging capability of hydroxyl radicals that oxidize DNA.

## Conclusion

It may be concluded that this study describes the efficient syntheses of BIMs from the condensation of indole with formylphenoxyacetic acid(s) in water in the absence of any catalyst. The formylphenoxyacetic acids behave as *in situ* Bronsted–Lowry acid catalysts in water. From the observation of single crystal X-ray analysis and DFT calculation, the two indole rings and the phenyl ring are found to be noncoplanar. All the synthesized compounds display  $\pi$ - $\pi^*$  transition and can potentially serve as photoactive materials. Theoretical calculations were used to obtain optimized structures as well as spatial distributions of the HOMO and LUMO levels of the compounds. Compounds have a better DPPH radical scavenging activity and a decrease in oxidative damage of DNA.

## Acknowledgements

One of the authors (G.S. Suresh Kumar) thanks Ms. K. Ramalakshmi, Plantation Products and Flavour Technology Department, Central Food Technological Research Institute, Council of Scientific and Industrial Research (CSIR), Mysore, India. CDRI, Lucknow, India is acknowledged for the spectral studies.

## Appendix A. Supplementary material

Supplementary data associated with this article can be found, in the online version, at <http://dx.doi.org/10.1016/j.saa.2013.12.017>.

## References

- [1] (a) J.K. Porter, C.W. Bacon, J.D. Robbins, D.S. Himmelsbach, H.C.J. Higman, *Agric. Food Chem.* 25 (1977) 88–93; (b) T. Osawa, M. Namiki, *Tetrahedron Lett.* 24 (1983) 4719–4722; (c) G. Bifulco, I. Bruno, R. Riccio, J. Lavayre, G.J. Bourdy, *Nat. Prod.* 57 (1994) 1254–1261; (d) R. Bell, S. Carmeli, N.J. Sar, *Nat. Prod.* 57 (1994) 1587–1590; (e) T.R. Garbe, M. Kobayashi, N. Shimizu, N. Takesue, M. Ozawa, H.J. Yukawa, *Nat. Prod.* 63 (2000) 596–598.
- [2] (a) M. Shirri, M.A. Zolfigol, H.G. Kruger, Z. Tanbakouchian, *Chem. Rev.* 110 (2010) 2250–2293; (b) G.S. Suresh Kumar, S. Kumaresan, A. Antony Muthu Prabhu, N. Bhuvanesh, P.G. Seethalakshmi, *Spectrochim. Acta A* 101 (2013) 254–263; (c) G.S. Suresh Kumar, S. Kumaresan, *Int. J. Curr. Chem.* 3 (3 & 4) (2012) 91–103; (d) G.S. Suresh Kumar, S. Kumaresan, C. Shiju, Bijoy Mohan Das, G. Anantharaj, S. Subramanian, *Int. J. Basic Appl. Chem. Sci.* 2 (2) (2012) 1–7; (e) G.S. Suresh Kumar, A. Antony Muthu Prabhu, S. Jegan Jeniffer, N. Bhuvanesh, P. Thomas Muthiah, S. Kumaresan, *J. Mol. Str.* 1047 (2013) 109–120.
- [3] (a) V. Bala, Y.S. Chhonker, S.R. Hashim, *Asian J. Chem.* 22 (5) (2010) 3447–3452; (b) G.S. Suresh Kumar, S. Kumaresan, *J. Chem. Sci.* 124 (4) (2012) 857–863; (c) G.S. Suresh Kumar, P.G. Seethalakshmi, N. Bhuvanesh, S. Kumaresan, *J. Mol. Str.* 1034 (2013) 302–309; (d) G.S. Suresh Kumar, P.G. Seethalakshmi, D. Sumathi, N. Bhuvanesh, S. Kumaresan, *J. Mol. Str.* 1035 (2013) 476–482; (e) G.S. Suresh Kumar, P.G. Seethalakshmi, N. Bhuvanesh, S. Kumaresan, *J. Mol. Str.* 1050 (2013) 88–96; (f) G.S. Suresh Kumar, A. Antony Muthu Prabhu, P.G. Seethalakshmi, N. Bhuvanesh, S. Kumaresan, *J. Mol. Str.* 1059 (2014) 51–60.

- [4] (a) M. Syamala, *Org. Prep. Proced. Int.* 41 (2009) 1–68;  
(b) Barry B. Toure, Dennis G. Hall, *Chem. Rev.* 109 (2009) 4439–4486.
- [5] S. Marc-Olivier, L. Chao-Jun, *Chem. Soc. Rev.* 41 (2012) 1415–1427.
- [6] R.N. Butler, A.G. Coyne, *Chem. Rev.* 110 (2010) 6302–6337.
- [7] (a) B. Kosar, C. Albayrak, C.C. Ersanli, M. Odabasoglu, O. Buyukgungor, *Spectrochim. Acta A* 93 (2012) 1–9;  
(b) M. Belletête, P.T. Boudreault, M. Leclerc, G. Durocher, *J. Mol. Struct. Theochem.* 962 (2010) 33–37;  
(c) M. Szafran, A. Katrusiak, Z. Dega-Szafran, I. Kowalczyk, *J. Mol. Struct.* 1031 (2013) 49–55.
- [8] M.J. Frisch, G.W. Trucks, H.B. Schlegel, G.E. Scuseria, M.A. Robb, J.R. Cheeseman, J.A. Montgomery, Jr., T. Vreven, K.N. Kudin, J.C. Burant, J.M. Millam, S.S. Iyengar, J. Tomasi, V. Barone, B. Mennucci, M. Cossi, G. Scalmani, N. Rega, G.A. Petersson, H. Nakatsuji, M. Hada, M. Ehara, K. Toyota, R. Fukuda, J. Hasegawa, M. Ishida, T. Nakajima, Y. Honda, O. Kitao, H. Nakai, M. Klene, X. Li, J.E. Knox, H.P. Hratchian, J.B. Cross, V. Bakken, C. Adamo, J. Jaramillo, R. Gomperts, R.E. Stratmann, O. Yazyev, A.J. Austin, R. Cammi, C. Pomelli, J.W. Ochterski, P.Y. Ayala, K. Morokuma, G.A. Voth, P. Salvador, J.J. Dannenberg, V.G. Zakrzewski, S. Dapprich, A.D. Daniels, M.C. Strain, O. Farkas, D.K. Malick, A.D. Rabuck, K. Raghavachari, J.B. Foresman, J.V. Ortiz, Q. Cui, A.G. Baboul, S. Clifford, J. Cioslowski, B.B. Stefanov, G. Liu, A. Liashenko, P. Piskorz, I. Komaromi, R.L. Martin, D.J. Fox, T. Keith, M.A. Al-Laham, C.Y. Peng, A. Nanayakkara, M. Challacombe, P.M.W. Gill, B. Johnson, W. Chen, M.W. Wong, C. Gonzalez, J.A. Pople, Gaussian, Inc., Wallingford, CT, 2004.
- [9] (a) A.D. Becke, *J. Chem. Phys.* 98 (1993) 5648–5652;  
(b) C. Lee, W. Yang, R.G. Parr, *Phys. Rev. B* 37 (1988) 785–789.
- [10] M.S. Blois, *Nature* 4617 (1958) 1199–1200.
- [11] K. Ramalakshmi, G. Hithamani, K.R. Asha, L.J. Mohan Rao, *Int. J. Food Sci. Technol.* 46 (2011) 109–115.
- [12] (a) L. Daniel, Y. Mao, U. Saffiotti, *Free Radic. Biol. Med.* (1995) 463–472. 14;  
(b) B. Stinefelt, S.S. Leonard, K.P. Blemings, X. Shi, H. Klandorf, *Ann. Clin. Lab. Sci.* 35 (1) (2005) 37–45.
- [13] (a) A. Corma, H. Garcia, *Chem. Rev.* 10 (2003) 4307–4365;  
(b) T. Akiyama, *Chem. Rev.* 107 (2007) 5744–5758.
- [14] (a) D. Maciejewska, I. Szpakowska, I. Wolska, M. Niemyjska, M. Mascini, M. Maj-Zurawska, *Bioelectrochemistry* 69 (2006) 1–9;  
(b) D. Maciejewska, I. Wolska, M. Niemyjska, P. Zero, *J. Mol. Str.* 753 (2005) 53;  
(c) M. Rasztańska, D. Maciejewska, M. Niemyjska, I. Wolska, M. Wloostowski, M. Rasztańska, *Z. Naturforsch* 59 (b) (2004) 1137–1142.
- [15] (a) R. Krishna, D. Velmurugan, G. Babu, P.T. Perumal, *Acta Crystallogr. C* 55 (1999) 75–82;  
(b) R. Krishna, D. Velmurugan, S. Shanmuga Sundara, *Acta Crystallogr. C* 55 (1999) IUC9900084.
- [16] M. Crisma, F. Formaggio, G. Valle, C. Toniolo, M. Saviano, R. Lacovino, L. Zaccaro, E. Benedetti, *Biopolymers* 42 (1997) 1–6.
- [17] R. Martinez, A. Espinosa, A. Tarraga, P. Molina, *Tetrahedron* 64 (2008) 2184–2191.
- [18] A. Sarkar, P. Banerjee, S.U. Hossain, S. Bhattacharya, S.C. Bhattacharya, *Spectrochim. Acta* 72A (2009) 1097–1102.
- [19] M. Karelson, V.S. Lobanov, R. Katrizky, *Chem. Rev.* 96 (1996) 1027–1044.
- [20] B. Lu, J. Zhang, J. Li, J. Yao, M. Wang, Y. Zou, S. Zhu, *Tetrahedron* 68 (2012) 8924–8930.